THE JOURNAL OF PHYSICAL CHEMISTRY A

Article

Cite This: J. Phys. Chem. A 2018, 122, 451−459

pubs.acs.org/JPCA

Reaction Mechanism of Organocatalytic Michael Addition of Nitromethane to Cinnamaldehyde: A Case Study on Catalyst Regeneration and Solvent Effects

Published as part of The Journal of Physical Chemistry virtual special issue "Manuel Yáñez and Otilia Mó Festschrift".

Katarzyna Świderek,[†] Alexander R. Nödling,[‡] Yu-Hsuan Tsai,[‡] Louis Y. P. Luk,*[,‡] and Vicent Moliner*[,†,§]

[†]Departament de Química Física i Analítica, Universitat Jaume I, 12071 Castellón, Spain

[‡]School of Chemistry, Cardiff University, CF10 3AT Cardiff, United Kingdom

[§]School of Chemistry, University of Bath, BA2 7AY Bath, United Kingdom

Supporting Information

ABSTRACT: The Michael addition of nitromethane to cinnamaldehyde has been computationally studied in the absence of a catalyst and the presence of a biotinylated secondary amine by a combined computational and experimental approach. The calculations were performed at the density functional theory (DFT) level with the M06-2X hybrid functional, and a polarizable continuum model has been employed to mimic the effect of two different solvents: dichloromethane (DCM) and water. Contrary to common assumption, the product-derived iminium intermediate was absent in both of the solvents tested. Instead, hydrating the C1−C2 double bond in the enamine intermediate directly yields the tetrahedral intermediate, which is key for forming the product and regenerating the catalyst. Enamine hydration is concerted and found to be rate-limiting in DCM but segregated into two non-rate-limiting steps when the solvent is replaced with water. However, further analysis revealed that the use of water as solvent also raises the energy barriers for other chemical steps, particularly the critical step of C−C bond formation between the iminium intermediate and nucleophile; this consequently lowers both the reaction yield and enantioselectivity of this LUMO-lowering reaction, as experimentally detected. These findings provide a logical explanation to why water often enhances organocatalysis when used as an additive but hampers the reaction progress when employed as a solvent.

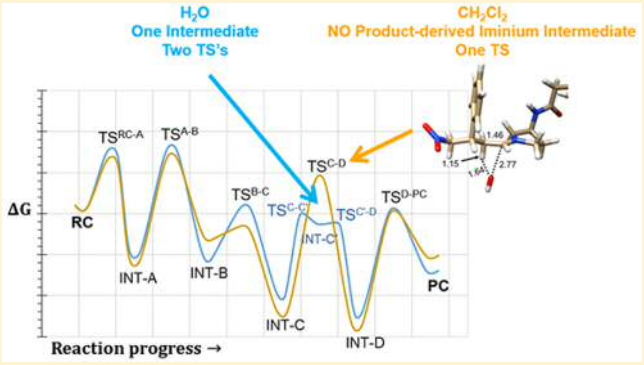

INTRODUCTION

Secondary amine organocatalysts have been widely used in organic synthesis as they are known to be multifunctional and able to mediate a plethora of chemical transformations.[1−3] Because they drive the progress of a reaction by inducing covalent intermediate formation, performing acid/base reaction, and controlling stereoselectivity via hydrogen bonding and steric effects, secondary amine organocatalysts are often referred to as the minimalist versions of enzymes.[3] However, unlike enzyme catalysis, many organocatalytic reactions cannot tolerate a reaction medium that contains a large degree of aqueous solvent.[1−3] This has consequently affected the development of many potential applications. Combining organocatalysts with enzymes in a one-pot multistep system, for example, has been considered as an efficient approach to produce chiral synthons with a minimal amount of solvent waste, but finding a compatible solvent system can be an extremely challenging task.[3−10] To this end, it is essential to elucidate the effect of solvents on organocatalysis by investigating the reaction mechanism.

The tolerance of a secondary amine organocatalytic reaction toward the presence of water greatly varies. It has been reported that pure water or buffer can be used for certain organocatalytic reactions,[11−14] whereas for others a solvent mixture containing different ratios of miscible organic solvent and water can be tolerated.[3,15−17] In fact, all chemical steps in a secondary amine organocatalytic reaction cycle can be affected by the presence of water. When a carbonyl substrate reacts with a secondary amine organocatalyst, an initial reactive iminium ion intermediate is formed. In the case where proline was used as the catalyst, the corresponding iminium intermediate can lead to the formation of an off-target parasitic

Received: November 30, 2017
Revised: December 18, 2017
Published: December 19, 2017

DOI: 10.1021/acs.jpca.7b11803
J. Phys. Chem. A 2018, 122, 451−459

species that can also be reversed by including water in the reaction.[18−20] On the other hand, water also disfavors the formation of the iminium intermediate, shifting the equilibrium toward the free catalyst.[3] It is also believed that the reaction cycle eventually leads to the formation of the second iminium intermediate, which upon hydrolysis yields the product and catalyst.[21,22] To the best of our knowledge, no studies have been performed to investigate the mechanism of product release, though it appears that the step of hydrolysis is likely favored by the presence of water.[21,22] Indeed, this may explain why previous kinetic investigations revealed that the step of product release becomes rate-limiting when water is completely removed from the reaction. Moreover, water greatly increases the dielectric constant of the reaction medium, which is suggested to perturb the energies of transition states (TSs) and stereoselectivity of the reaction.[3] Even though solvent screening is often done on a trail-and-error basis when a new reaction is performed,[3] a thorough study that analyzes the effect of water on organocatalysis has not been achieved.

Density functional theory (DFT) has been widely used in the mechanistic investigations of organocatalysis.[22−25] The substrate-derived iminium ion intermediate and the TSs localized in the gas phase have been analyzed to explain the stereoselectivity of chiral imidazolidinones and pyrrolidines.[22,23,26−28] However, the solvent effect on organocatalysis has not been interrogated in this manner. Furthermore, to the best of our knowledge, the full reaction process including the mechanism of product release in any of the secondary amine organocatalyses has not been investigated. Here, the Michael addition of nitromethane to α,β-unsaturated aldehyde catalyzed by a pyrrolidine-derived organocatalyst has been investigated at the DFT level with a polarizable continuum model to mimic the effect of dichloromethane (DCM) and aqueous solution (Scheme 1). The aim of this work is to elucidate the molecular mechanism of this LUMO-lowering reaction and to analyze how a change of the reaction medium affects the efficiency of organocatalysis.

Scheme 1. Organocatalytic Michael Addition of Nitromethane to Cinnamaldehyde

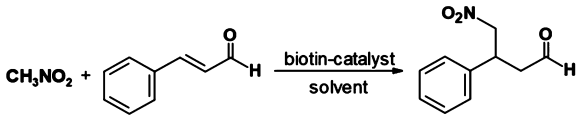

COMPUTATIONAL METHODS

Pyrrolidine-derived organocatalysts often contain bulky or hydrogen-bonding substituent groups at the carbons adjacent to the reacting nitrogen.[29−35] The physical properties of these substituents can affect the step of product hydrolysis. In order to exclude these effects, we did not choose a popular system, i.e., Jørgensen−Hayashi or MacMillan catalysts,[1−3] but a simple 3-aminoproline derivative coupled to biotin at the C-3 position. This would allow better solubility in water in comparative experimental studies. Hence, the present theoretical study has been performed with the molecular model of an organocatalytic LUMO-lowering reaction where a biotin moiety was added to the C-3 position of the pyrrolidine catalyst via an amide linkage (Figure 1). The potential energy surfaces (PESs) for the Michael addition of nitromethane to cinnamaldehyde have been obtained at the DFT level with the M06-2X hybrid functional[36,37] and the 6-31+G(d,p) basis set, following the suggestions of Truhlar and co-workers for studies of main-group thermochemistry and kinetics[36] to get an appropriate accuracy in relative energies.[38] Recent studies on reactivity carried out in our laboratories also support the selection of this combination of functional and basis set for reactions in enzymes[39−42] and in solution.[43] The effect of the solvent was introduced by means of a solute electron density model (SMD) developed by Truhlar and co-workers.[44] Once the first-order saddle points were located and characterized, the intrinsic reaction coordinate (IRC) path was traced down from the saddle points to the corresponding minima using the full gradient vector. The global rms residual gradient in the optimized structures was always less than 0.04 kcal mol^{-1} Å^{-1}. It is important to note that no constraints were applied to any of the geometry optimizations. In order to avoid possible artifacts, such as odd interaction complexes, defining a proper orientation in the starting point structures is a crucial step. Also, keeping in mind that the reaction under study is a multistep process, the IRC calculations traced forward from a TS structure do not necessarily converge in the end of the backward path traced from the following IRC. Efforts have therefore been made to get a converged intermediate result from consecutive steps of the reaction path. Zero-point energies and thermal contributions to the enthalpy and to

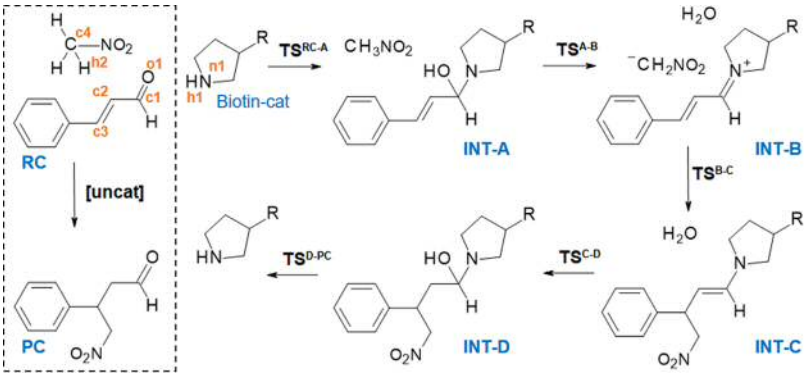

Figure 1. Schematic representation of the reactants complex (RC), products complex (PC), and intermediate states located along the catalyzed Michael addition of nitromethane to cinnamaldehyde in DCM. R = NH-biotin. The direct noncatalyzed reaction from **RC** to **PC** is indicated in the dashed rectangle. Labels of key atoms are shown in the **RC** panel.

DOI: 10.1021/acs.jpca.7b11803
J. Phys. Chem. A 2018, 122, 451−459

Table 1. Key Interatomic Distances (in Å) of the Stationary Point Structures along the Catalyzed Michael Addition of Nitromethane to Cinnamaldehyde Obtained in (a) DCM and in (b) Aqueous Solution at the M06-2X/6-31+G(d,p) Level

(a) DCM											
	RC	TS^{RC-A}	INT-A	TS^{A-B}	INT-B	TS^{B-C}	INT-C	TS^{C-D}	INT-D	TS^{D-PC}	PC
n1−h1	1.03	1.23	2.33	3.17	3.91	4.23	5.42	4.25	2.63	1.22	1.02
h1−o1	2.43	1.33	0.97	0.97	0.96	0.98	0.97	0.96	0.97	1.36	2.55
o1−c1	1.30	1.38	1.42	1.89	3.34	4.52	4.42	2.77	1.43	1.37	1.28
c1−n1	1.66	1.53	1.45	1.33	1.29	1.32	1.36	1.29	1.44	1.53	1.70
o1−h2	2.23	2.21	3.30	1.18	0.99	0.97	0.97	1.64	2.63	2.69	2.68
h2−c4	1.09	1.09	1.09	1.44	3.84	3.24	2.92	2.74	2.91	2.64	2.66
h2−c2	4.59	4.05	3.86	3.28	3.56	3.41	3.15	1.15	1.10	1.10	1.10
c3−c4	6.47	6.07	5.00	4.31	5.76	2.91	1.55	1.53	1.54	1.53	1.53
(b) Aqueous Solution											
	RC	TS^{RC-A}	INT-A	TS^{A-B}	INT-B	TS^{B-C}	INT-C	$TS^{C-C'}$	INT-C′	$TS^{C'-D}$	INT-D	TS^{D-PC}	PC
n1−h1	1.03	1.24	2.51	2.86	5.76	2.77	3.12	4.67	3.46	3.42	2.56	1.25	1.02
h1−o1	2.45	1.31	0.97	0.97	0.96	0.97	0.97	0.97	0.96	0.97	0.97	1.31	2.38
o1−c1	1.33	1.40	1.42	1.62	5.00	3.41	3.24	3.36	2.82	2.49	1.42	1.40	1.33
c1−n1	1.58	1.52	1.46	1.38	1.29	1.32	1.37	1.29	1.28	1.29	1.45	1.51	1.58
o1−h2	3.02	3.20	3.25	1.08	0.99	0.97	0.97	1.46	3.10	2.84	2.52	2.70	2.59
h2−c4	1.09	1.09	1.09	1.61	2.81	3.00	2.99	2.70	2.68	2.66	2.66	2.64	2.64
h2−c2	2.93	3.11	3.19	2.87	3.52	2.93	2.46	1.23	1.10	1.10	1.10	1.09	1.10
c3−c4	3.54	3.52	3.62	4.00	3.85	2.22	1.54	1.52	1.53	1.53	1.53	1.53	1.53

the free energy were obtained at 298 K by means of the M06-2X functional within the rigid-rotor and harmonic approximation in the gas phase.[45] Natural population analysis has been performed for all stationary structures.[46] Time-dependent DFT (TDDFT) calculations were used for performing the frontier orbital analysis. All calculations were performed with Gaussian 09, version A.[47]

EXPERIMENTAL METHODS

Catalytic Reactions in Different Solvents. The formate salt of the biotinylated organocatalyst (35.8 mg, 0.1 mmol, 0.2 equiv) was dissolved in the respective solvent (1.0 mL) in a glass vial. Nitromethane (268 μL, 5.0 mmol, 10.0 equiv) and cinnamaldehyde (63 μL, 0.5 mmol, 1.0 equiv) were added. The mixture was stirred for 22 h (26 h in the case of water as the solvent) at 25 °C. In the case of water as the solvent, the aqueous phase was extracted with $CDCl_3$ (1.0 mL), and 0.1 mL of this solution was transferred into an NMR tube containing $CDCl_3$ (0.9 mL). In the case of organic solvents (DCM or MeOH), the solvent used in the reaction was removed under reduced pressure. The respective residue was taken up in $CDCl_3$ (1.0 mL), and 0.1 mL of this solution was transferred into an NMR tube containing $CDCl_3$ (0.9 mL). The diluted samples were directly subjected to ^1H NMR analysis. The yield was determined by comparing the integrals of the aldehyde protons, the double bond proton, and the newly formed α-carbonyl protons (see Supporting Information).

Determination of the Enantioselectivities. In order to determine the enantioselectivity, 0.4 mL of the undiluted $CDCl_3$ solution of the crude material was purified by preparative TLC (*n*-hexane:EtOAc 75:25) using a complete sheet. The part containing product **PC** (checked via a racemic reference sample by UV fluorescence deletion and permanganate stain) was cut out. The silica scratched from the aluminum plate was stirred in DCM for several minutes. The silica was filtered off and washed with DCM, and the filtrate was concentrated under reduced pressure. Purified **PC** was dissolved in about 3.0 mL of MeOH, sodium borohydride (20 mg, 0.53 mmol) was added, and the mixture was stirred for 2 h. Deionized water (5 mL) and DCM (5 mL) were added, and the pH was carefully adjusted to 6.0 with 0.1 M hydrochloric acid. The aqueous phase was extracted with DCM (3 × 10 mL), and the combined organic phases were dried over $MgSO_4$ and concentrated under reduced pressure. The crude material was purified by preparative TLC (*n*-hexane:EtOAc 66:33) using a complete sheet. The part containing **reduced** product **RPC** (checked via a racemic reference sample by UV fluorescence deletion and permanganate stain; see the Supporting Information) was cut out. The silica scratched from the aluminum plate was stirred in DCM for several minutes. The silica was filtered off and washed with DCM, and the filtrate was concentrated under reduced pressure. The residue was dissolved in *n*-hexane:*i*PrOH 80:20 and the sample analyzed via chiral HPLC.

RESULTS AND DISCUSSION

Deduced at the M06-2X level, a schematic representation of the different stable species that appear along the Michael addition of nitromethane to cinnamaldehyde in both DCM and water is depicted in Figure 1. The key interatomic distances of the optimized structures are listed in Table 1.

As shown in Figure 1, the catalyzed reaction in DCM takes place in five steps that begins with the nucleophilic attack of the nitrogen atom in the pyrrolidine to the C1 atom of the carbonyl group in cinnamaldehyde, concomitant with proton transfer from the nitrogen atom to the carbonyl oxygen atom of the aldehyde motif. In the second step, the hydroxyl group of the newly generated tetrahedral species INT-A abstracts a proton from nitromethane, generating a water molecule and an ion pair that contains the iminium intermediate INT-B. Subsequently, a C−C bond is formed between the two ionized molecules, yielding the enamine INT-C. Asynchronous proton transfer and nucleophilic attack of a water molecule on the C1−C2 double bond (i.e., hydration) results in the second tetrahedral intermediate INT-D. This water molecule used in

DOI: 10.1021/acs.jpca.7b11803
J. Phys. Chem. A 2018, 122, 451−459

the step of hydration originates from the formation of the iminium ion intermediate during the simulations. A note of caution must be taken because this approximation does not necessarily represent the real situation where the substrate is surrounded by a non-negligible number of undistinguishable water molecules (when the reaction was studied in aqueous solution or in "wet" DCM). Even though an entropic term can be lost within the calculation, the potential energy profile is unlikely to be dramatically affected. Last, the carbon−nitrogen bond that links the product and the pyrrolidinyl ring is broken, thereby releasing the product and regenerating the catalyst for another cycle of reaction. Notably, the commonly assumed product-derived iminium intermediate was not observed. Hence, hydrating the double bond of enamine INT-C has become an essential step toward forming the production and regenerating the catalyst.

The reaction mechanism deduced from our calculations is in agreement with some of the findings made in the previous works on related reactions. For instance, the iminium ion intermediate INT-B was also detected by Platts, Tomkinson and co-workers as a key reactive intermediate.[21,48−50] Some discrepancies however were also observed. Previously, the mechanistic studies of secondary amine-catalyzed Diels−Alder reaction showed a three-step process instead of a five-process as observed here.[21,48−50] Formation of the reactive iminium ion INT-B by the condensation of the catalyst with the α,β-unsaturated carbonyl substrate takes place in two steps rather than a concerted manner. Similarly, subsequent to the step of C−C bond formation (the Michael addition in our case or a Diels−Alder reaction), regeneration of the catalyst via hydrolysis proceeds in two steps rather in a single step as previously predicted.[21,48−50]

The free energy profiles of the reactions in DCM and in aqueous solution are shown in Figure 2, while the

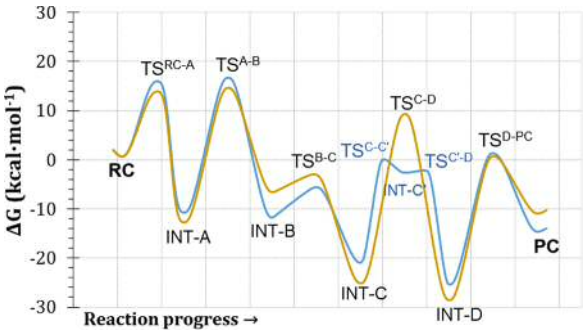

Figure 2. M06-2X/6-31+G(d,p) free energy profiles for the catalyzed Michael addition of nitromethane to cinnamaldehyde obtained in DCM (orange line) and in aqueous solution (blue line).

corresponding energies of all of the species relative to RC are provided in Table 2. The comparison with the relative potential energies shows how the vibrational corrections diminish the barrier heights (Table S1). Analysis of the free energy profiles obtained in the two solvent systems reveals a difference in the reaction mechanism. The reaction in DCM takes place in five steps, while there are six steps for the reaction conducted in aqueous solution because the molecular mechanisms used in hydrating the enamine INT-C are different. The attack of the oxygen atom in the water molecule on C1 and the step of proton transfer to C2 take place concertedly in DCM. In contrast, the aqueous medium

Table 2. Relative Free Energies (in kcal·mol^{-1}) of the Stationary Point Structures Appearing along the Catalyzed Michael Addition of Nitromethane to Cinnamaldehyde Obtained at the M06-2X/6-31+G(d,p) Level in DCM and in Water

	ΔG/kcal·mol^{-1}		
chemical species	DCM	water	
RC	0.0	0.0	
TS^{RC-A}	14.3	16.3	
INT-A	−13.1	−11.1	
TS^{A-B}	15.0	17.1	
INT-B	−6.8	−12.1	
TS^{B-C}	−2.6	−5.2	
INT-C	−25.4	−21.2	
TS^{C-D}	9.6	$TS^{C-C'}$	0.2
		INT-C′	−2.6
		$TS^{C'-D}$	−2.1
INT-D	−28.9	−25.7	
TS^{D-PC}	1.1	1.6	
PC	−11.2	−25.1	

stabilizes the hydroxyl anion after transferring the proton to C2, thereby generating a metastable intermediate INC-C′ (Figures 2 and 3). This additional step significantly decreases the effective free energy barrier for the formation of INT-D (35.0 and 21.4 kcal·mol^{-1} in DCM and water, respectively). This result is in agreement with the previous experimental observations that indicate that the step of hydrolysis is favored by the presence of water.[21,22] The rest of the chemical steps are comparable in both media but present slightly higher energy TSs in water than in DCM (Figure 2 and Table 2), highlighting the advantage of using an organic solvent to progress the reaction cycle. In the reaction performed in DCM, the TS corresponding to the attack of the pyrrolidine catalyst on the aldehyde motif (TS^{RC-A}) is only 0.7 kcal·mol^{-1} lower than the TS corresponding to the formation of the reactive ion pair (TS^{A-B}). However, the free energy required to form the TS^{A-B} species from INT-A (28.1 kcal·mol^{-1}) is noticeably higher than that to yield TS^{RC-A} from the reactant (14.3 kcal·mol^{-1}). The critical C−C bond formation between the nitromethane anion and the iminium ion in INT-B (TS^{B-C}) is clearly not rate-limiting, showing a free energy barrier of only 4.2 kcal·mol^{-1}; however, in water, the barrier of this step is higher (6.9 kcal·mol^{-1}). The progress of the organocatalytic reaction in DCM is likely kinetically controlled by the formation of TS^{C-D} (35 kcal·mol^{-1}). On the other hand, in water, converting INT-C to INT-D requires 21.4 kcal·mol^{-1}, which is lower than the barrier for forming the ion pair INT-B (28.2 kcal·mol^{-1}). Accordingly, the nucleophilic attack of the C−C double bond on the water molecule is likely rate-limiting in DCM, while in water, ionization of the nitromethane concomitant with the formation of the iminium intermediate (step from INT-A to INT-B) would present the highest free energy barrier (28.2 kcal·mol^{-1}).

Inspection of the five TS structures obtained in DCM provides additional mechanistic insights (Figure 3). The first TS species TS^{RC-A} clearly shows a four-membered ring where the attack of the nitrogen atom of the pyrrolidine ring on the carbonyl group in cinnamaldehyde and the H1 proton transfer between the N and O atoms take place concertedly. Formation of the iminium cation via TS^{A-B} appears to be in an advanced stage of the process; it confirms the formation of the double

DOI: 10.1021/acs.jpca.7b11803
J. Phys. Chem. A 2018, 122, 451−459

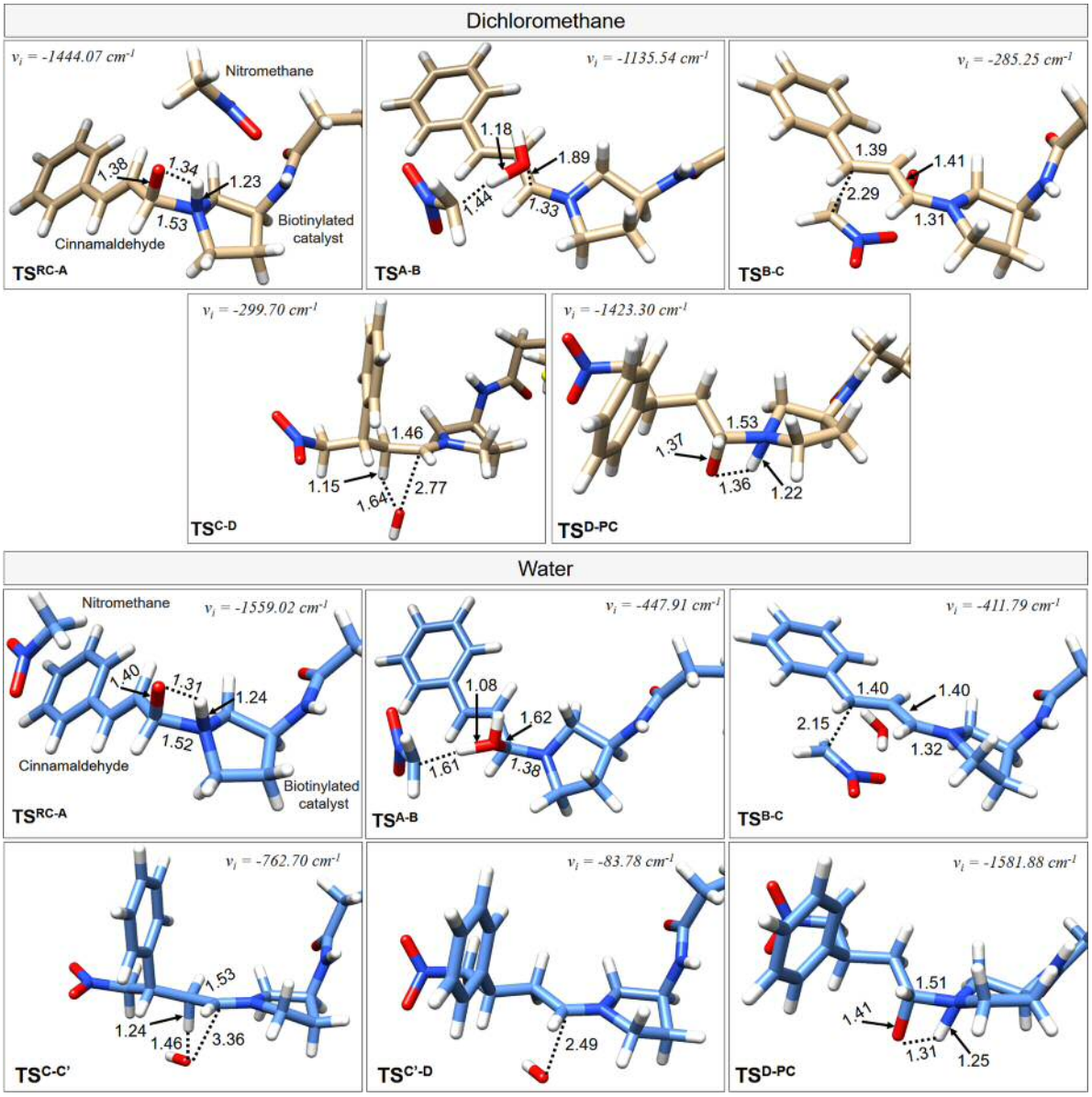

Figure 3. Representation of the TS structures obtained along the reaction coordinate of the catalyzed Michael addition of nitromethane to cinnamaldehyde in DCM and in water. Key interatomic distances are reported in Å, while imaginary frequencies are reported in cm^{-1}.

bond between C1 and N1 and an almost-transferred proton from the C4 atom of the nitromethane to the O1 atom of the original cinnamaldehyde with the C−O bond nearly broken at the 1 position. The last step corresponding to the formation of the product is equivalent to the reverse reaction of the first step where the bond between the substrate and the catalyst was formed. Consequently, TS^{RC-A} and TS^{D-PC} are essentially equivalent (Figure 3), and the interatomic distances are similar in these two structures (Table 1). Accordingly, the free energy barrier from INT-D to TS^{D-PC} is nearly coincident with the free energy barrier from INT-A to TS^{RC-A} (30.0 and 27.3 kcal·mol^{-1}, respectively). The small discrepancy between them is likely due to the slightly different conformers obtained during the optimizations. Analysis of the TS structures located along the reaction in aqueous solution (see Figure 3) are qualitatively equivalent to those located in DCM, except that two new TSs, $TS^{C-C'}$ and $TS^{C'-D}$, appear during the transformation from INT-C to INT-D. As mentioned above, the polar environment of the aqueous solution stabilized the hydroxyl group that is formed after the reactive water molecule transferred a proton to the C2 carbon atom.

Uggerud and co-workers carried out a quantum chemical study of both the catalyzed and noncatalyzed nucleophilic addition of nitromethane to α,β-unsaturated carbonyl compounds in the gas phase.[51] Their results indicated that the formation of the iminium ion would be the rate-limiting step. Moreover, they identified a cyclic isoxazolidine that results from the nucleophilic attack of the double bond intermediate, but such an intermediate was not detected in our simulations. These discrepancies suggest that our calculated reaction proceeds through a different reaction mechanism. This can be caused by the slight variations between the secondary amine organocatalysts used or the fact that the present study takes the solvent effect into account.

The direct transformation from reactants to products without the participation of the pyrrolidine (**RC** to **PC** in Figure 1) is considered as the model of the uncatalyzed reaction in solution. The exploration of this reaction by

DOI: 10.1021/acs.jpca.7b11803
J. Phys. Chem. A 2018, 122, 451−459

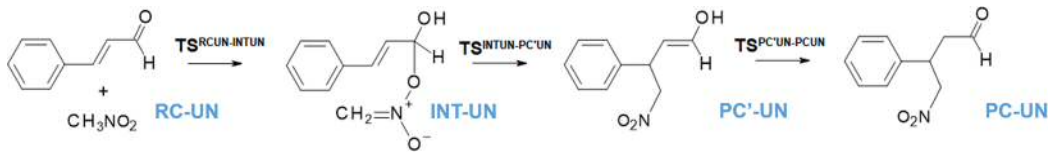

Figure 4. Schematic representation of the reaction mechanism of the noncatalyzed Michael addition of nitromethane to cinnamaldehyde in DCM.

quantum mechanical DFT methods has revealed that the reaction does not take place in a single step but in a stepwise manner in both water and DCM (Figure 4). In the first step of the reaction in both of the solvents, the oxygen atom in nitromethane attacks the carbonyl motif of cinnamaldehyde, generating a stable intermediate, INT-UN. Interestingly, as observed in Figure 6, the C−O forming bond at the $TS^{RCUN-INTUN}$ is at an earlier stage of the process in water than that in DCM, likely because the latter provides a highly polar environment to stabilize the nitro group. The second step corresponds to an intramolecular aldol reaction that produces an enol intermediate **PC′**-UN, which transforms into the product **PC**-UN. As reported in Table 3 and Figure 5, there is

Table 3. Relative Free Energies (in kcal·mol^{-1}) of the Stationary Point Structures Appearing along the Noncatalyzed Michael Addition of Nitromethane to Cinnamaldehyde Obtained at the M06-2X/6-31+G(d,p) Level in DCM and in Water

	ΔG/kcal·mol^{-1}	
chemical species	DCM	Water
RC-UN	0.0	0.0
$TS^{RCUN-INTUN}$	39.1	31.2
INT-UN	11.8	11.2
$TS^{INTUN-PC'UN}$	38.1	30.5
PC′-UN	−6.2	−6.0
$TS^{PC'UN-PCUN}$	53.2	53.6
PC	−15.7	−16.8

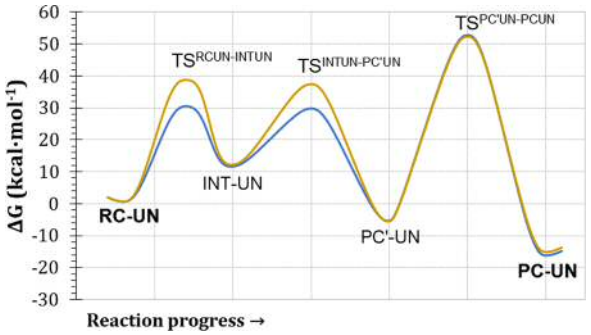

Figure 5. Free energy profile for the uncatalyzed Michael addition of nitromethane to cinnamaldehyde obtained in DCM (orange line) and in aqueous solution (blue line).

a significantly high energy barrier for this last step in both of the solvents (ca. 60 kcal·mol^{-1}) that corresponds to the step of tautomerization (see Figure 4). As shown in Figure 6, the TS structure of this step, $TS^{PC'UN-PCUN}$, involves the formation of an unfavorable intramolecular four-membered ring. The attack of the nitromethane and the noncatalyzed intramolecular aldol addition is also energetically demanding. In DCM, formation of $TS^{RCUN-INTUN}$ and $TS^{INTUN-PC'UN}$ requires relative energies of 39.1 and 38.1 kcal·mol^{-1}, respectively; in aqueous solution,

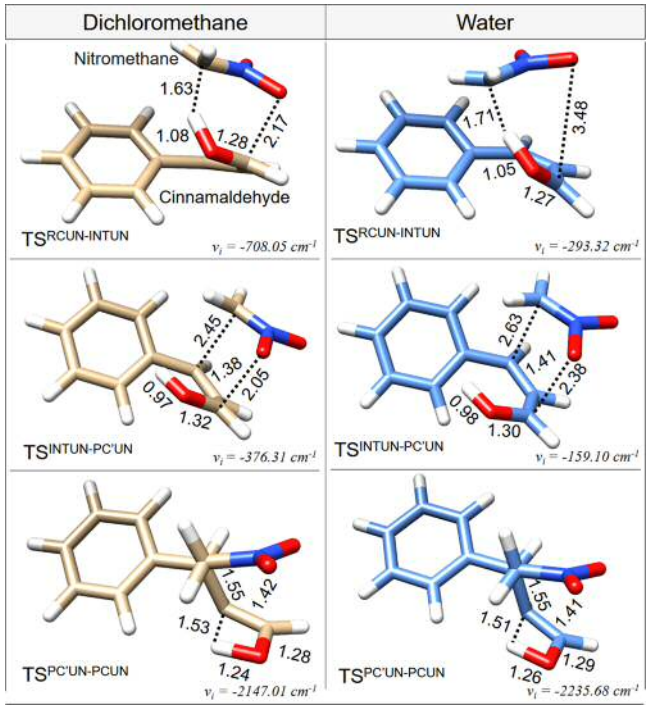

Figure 6. Representation of the TS structures obtained along the reaction coordinate of the uncatalyzed Michael addition of nitromethane to cinnamaldehyde in DCM and in water. Key interatomic distances are reported in Å, while imaginary frequencies are reported in cm^{-1}.

the corresponding relative energies are 31.2 and 30.5 kcal·mol^{-1}, respectively. It should be noted that, in the secondary amine-catalyzed reaction the corresponding C−C bond formation involves a relatively stable intermediate INT-B (−6.8 and −12.1 kcal·mol^{-1} in DCM and water, respectively), and formation of TS^{B-C} has a barrier of only 4.2 kcal·mol^{-1} in DCM and 6.9 kcal·mol^{-1} in water (see Figure 2 and Table 1), which are dramatically lower than the values for the corresponding steps of the uncatalyzed reaction. This highlights the catalytic effect of the secondary amine along the full reaction process.

Frontier Orbital Analysis. A molecular orbital analysis, with the TDDFT method at the M06-2X/6-31G(d,p) level, has been carried out to explore the electronic effects of the catalyst and the solvent on the frontier orbitals. The highest occupied molecular orbital (HOMO) and the lowest unoccupied molecular orbital (LUMO) have been computed for the isolated cinnamaldehyde and the iminium intermediate INT-B. The energy gap between the HOMO and LUMO of the cinnamaldehyde has been narrowed upon forming the iminium intermediate in both solvents (Figure 7). For the reaction in DCM, the difference decreases from 4.45 to 3.87 eV (a difference of 0.58 eV), whereas in aqueous solution, the decrease in the energy gap is from 3.82 to 2.96 eV (a difference of 0.86 eV). This therefore suggests that a polar environment

DOI: 10.1021/acs.jpca.7b11803
J. Phys. Chem. A 2018, 122, 451−459

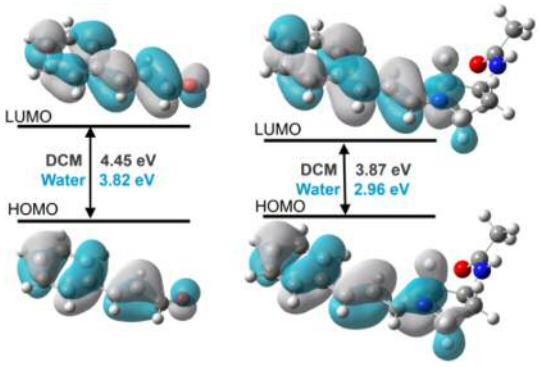

Figure 7. Frontier orbital representation of isolated cinnamaldehyde (left) and the iminium intermediate, INT-B (right). Results computed with TDDFT at the M06-2X/6-31G(d,p) level in DCM and in water.

causes a stronger electrostatic effect on the frontier orbitals. However, the energy barrier that converts INT-B to INT-C was found to be higher in water than that in DCM, thus indicating that the effect of the solvent on the reactivity corresponding to the step of Michael addition cannot be described entirely based on the energy gap between the HOMO and LUMO. By comparing the effect of adding the biotin fragment, the reactivity on the carbon−carbon double bond is significantly enhanced in the corresponding iminium intermediate (right panel in Figure 7) when compared to that of the isolated cinnamaldehyde (left panel in Figure 7); the nucleophilic attack at the C3 position is therefore enhanced in the presence of the biotinylated catalyst. In agreement with the calculations above, the barrier for the step of nucleophilic attack is only 3.7 kcal·mol^{-1} for the catalyzed reaction, while the corresponding reaction barrier of the uncatalyzed reaction is significantly higher (>30 kcal·mol^{-1}). Furthermore, while the HOMO of the isolated cinnamaldehyde involves conjugation of the C1−C2−C3 atoms, the HOMO of the iminium intermediate is more concentrated on the reactive C2−C3 double bond.

Experimental Observations. The catalyst was experimentally prepared, and the modeled organocatalytic reaction was performed in water, methanol, and DCM. In the absence of the catalyst, the formation of product was negligible (<2%), confirming that there is a high reaction barrier. When the catalyst is included, the reaction yield increases by 2- to 4-fold. The yield in the protic solvents is significantly lower than that in the aprotic counterpart (Table 4). Also, enantioselectivity is only observed when DCM is used, whereas it is negligible in the reactions conducted in water and methanol. Moreover, the use of methanol induces the formation of a byproduct where the nucleophilic attack takes place at the C2 position of cinnamaldehyde.

Table 4. Reaction Yields and Enantiomeric Ratios of the Model Reactions[a]

entry	solvent	yield (%)	enantiomeric ratio (R:S)	comment
1	water	3[b]	53:47	• negligible enantioselectivity
2	methanol	5	55:45	• 7% of the 1,2-addition product observed • nearly negligible enantioselectivity
3	dichloromethane	12	68:32	• mild enantioselectivity

[a]Conditions: 0.5 mmol cinnamaldehyde, 5 mmol nitromethane, 0.1 mmol biotinylated catalyst, 1 mL solvent, 25 °C, 22 h. [b]26 h reaction time.

CONCLUSIONS

The Michael addition of nitromethane to cinnamaldehyde has been computationally studied in the absence of a catalyst and the presence of a biotinylated secondary amine. The uncatalyzed reaction employs a completely different reaction mechanism, and the free energy barriers are noticeably higher. Our results also confirm that the secondary amine catalyst is capable of narrowing the energy gap between the HOMO and LUMO of α,β-unsaturated carbonyl substrates, thereby diminishing the energy barrier for the step of C−C bond formation. Contrary to conventional assumption, the product-derived iminium intermediate is absent in the calculated reaction pathway. Instead, the product-derived tetrahedral intermediate is directly formed by hydrating the enamine intermediate. This therefore rules out the hypothesis that water reacts with the product-derived iminium intermediate and induces the steps of product hydrolysis and catalyst regeneration.

The reaction mechanism was also found to be dependent on the solvent used. In the reaction performed in DCM, the step of nucleophilic attack by water on the C−C double bond is rate-limiting. When the organic solvent is replaced by water, this chemical transformation is separated into two steps, where the aqueous medium stabilizes the hydroxyl group of the reacting water after transferring the proton to C2 and generating a metastable intermediate. This consequently lowers the free energy barrier, and formation of the initial iminium intermediate becomes rate-limiting. As illustrated by the experimental studies, however, the reaction performed in water is not superior to that conducted in DCM, which gives a higher reaction yield and better stereoselectivity. A logical explanation to such an observation can be derived by comparing the free energy profiles of the reaction pathways. Although the step of nucleophilic attack by water is not rate-limiting in the aqueous solution, the energies of other TSs are higher. Noticeably, the critical C−C bond formation between the deprotonated nitromethane and the iminium ion in INT-B (TS^{B-C}) is significantly higher in water. Together, these steps likely contribute to a lower reaction rate in the aqueous solution. Furthermore, water may interact with the intermediates and is known to form nonreactive acetal intermediates with aldehyde;[50] these factors likely stall the reaction progress and hamper the stereoselectivity. Our results also help explain why many organocatalytic reactions performed best in organic solvent that is added with a stoichiometric amount of water.[1−3] Such an environment maintains lower energy barriers for most chemical steps; meanwhile, there is sufficient amount of water to drive the hydration step of the enamine intermediate but not enough to hamper the reaction progress and stereoselectivity. In summary, the results derived from this work will pave the way for designing a medium suitable for organocatalysis.

ASSOCIATED CONTENT

Supporting Information

The Supporting Information is available free of charge on the ACS Publications website at DOI: 10.1021/acs.jpca.7b11803.

DOI: 10.1021/acs.jpca.7b11803
J. Phys. Chem. A 2018, 122, 451−459

Relative potential energies of the stationary point structures appearing along the catalyzed and the uncatalyzed Michael addition of nitromethane to cinnamaldehyde; total potential energies of **RC**s in DCM and in water; NMR of the catalyst and reaction progress; chiral LC analysis; and complete ref 47 (PDF)

AUTHOR INFORMATION

Corresponding Authors

*E-mail: LukLY@cardiff.ac.uk (L.Y.P.L.).
*E-mail: moliner@uji.es (V.M.).

ORCID

Katarzyna Świderek: 0000-0002-7528-1551
Alexander R. Nödling: 0000-0002-3483-6266
Yu-Hsuan Tsai: 0000-0003-0589-5088
Louis Y. P. Luk: 0000-0002-7864-6261
Vicent Moliner: 0000-0002-3665-3391

Notes

The authors declare no competing financial interest.

ACKNOWLEDGMENTS

This computational work was supported by the Spanish Ministerio de Economía y Competitividad (Project CTQ2015-66223-C2), Generalitat Valenciana (PROMETEOII/2014/022), Universitat Jaume I (Project P1·1B2014-26), and the U.S. National Institutes of Health (Ref No. NIH R01 GM065368). V.M. is grateful to the University of Bath for the award of a David Parkin Visiting Professorship and to the Spanish Ministerio de Educación Cultura y Deporte for travel financial support (Project PRX17/00166). The authors acknowledge computational resources from the Servei d'Informàtica of Universitat Jaume I. The experimental work is supported by the startup fund provided by the Cardiff School of Chemistry, the Leverhulme Trust through a grant to L.Y.P.L (RPG-2017-195), and the Wellcome Trust through grants to L.Y.P.L (202056/Z/16/Z) and to Y.H.T (200730/Z/16/Z). We would like to thank Dr. Louis Morrill for the helpful discussion and allowing us to use their chiral LC.

REFERENCES

(1) *Asymmetric Organocatalysis 1*; List, B., Ed.; Thieme: Stuttgart, Germany, 2012; Vol. *1*.
(2) *Comprehensive Enantioselective Organocatalysis: Catalysts, Reactions, and Applications*; Dalko, P. I., Ed.; Wiley-VCH Verlag GmbH & Co. KGaA: Weinheim, Germany, 2013.
(3) Jimeno, C. Water in asymmetric organocatalytic systems: a global perspective. *Org. Biomol. Chem.* **2016**, *14*, 6147−6164.
(4) Baer, K.; Kraußer, M.; Burda, E.; Hummel, W.; Berkessel, A.; Gröger, H. Sequential and Modular Synthesis of Chiral 1,3-Diols with Two Stereogenic Centers: Access to All Four Stereoisomers by Combination of Organo- and Biocatalysis. *Angew. Chem., Int. Ed.* **2009**, *48*, 9355−9358.
(5) Rulli, G.; Duangdee, N.; Baer, K.; Hummel, W.; Berkessel, A.; Gröger, H. Direction of Kinetically versus Thermodynamically Controlled Organocatalysis and Its Application in Chemoenzymatic Synthesis. *Angew. Chem., Int. Ed.* **2011**, *50*, 7944−7947.
(6) Kinnell, A.; Harman, T.; Bingham, M.; Berry, A.; Nelson, A. Development of an organo- and enzyme-catalysed one-pot, sequential three-component reaction. *Tetrahedron* **2012**, *68*, 7719−7722.
(7) Heidlindemann, M.; Rulli, G.; Berkessel, A.; Hummel, W.; Gröger, H. Combination of Asymmetric Organo- and Biocatalytic Reactions in Organic Media Using Immobilized Catalysts in Different Compartments. *ACS Catal.* **2014**, *4*, 1099−1103.
(8) Gröger, H.; Hummel, W. Combining the 'two worlds' of chemocatalysis and biocatalysis towards multi-step one-pot processes in aqueous media. *Curr. Opin. Chem. Biol.* **2014**, *19*, 171−179.
(9) Suljić, S.; Pietruszka, J.; Worgull, D. Asymmetric Bio- and Organocatalytic Cascade Reaction − Laccase and Secondary Amine-Catalyzed α-Arylation of Aldehydes. *Adv. Synth. Catal.* **2015**, *357*, 1822−1830.
(10) Bisogno, F. R.; López-Vidal, M. G.; de Gonzalo, G. Organocatalysis and Biocatalysis Hand in Hand: Combining Catalysts in One-Pot Procedures. *Adv. Synth. Catal.* **2017**, *359*, 2026−2049.
(11) Torii, H.; Nakadai, M.; Ishihara, K.; Saito, S.; Yamamoto, H. Asymmetric Direct Aldol Reaction Assisted by Water and a Proline-Derived Tetrazole Catalyst. *Angew. Chem., Int. Ed.* **2004**, *43*, 1983−1986.
(12) Zheng, Z.; Perkins, B. L.; Ni, B. Diarylprolinol Silyl Ether Salts as New, Efficient, Water-Soluble, and Recyclable Organocatalysts for the Asymmetric Michael Addition on Water. *J. Am. Chem. Soc.* **2010**, *132*, 50−51.
(13) Palomo, C.; Landa, A.; Mielgo, A.; Oiarbide, M.; Puente, A.; Vera, S. Water-compatible iminium activation: organocatalytic Michael reactions of carbon-centered nucleophiles with enals. *Angew. Chem., Int. Ed.* **2007**, *46*, 8431−8435.
(14) Raj, M.; Singh, V. K. Organocatalytic reactions in water. *Chem. Commun.* **2009**, 6687−6703.
(15) Paras, N. A.; MacMillan, D. W. C. New Strategies in Organic Catalysis: The First Enantioselective Organocatalytic Friedel−Crafts Alkylation. *J. Am. Chem. Soc.* **2001**, *123*, 4370−4371.
(16) Chen, X.-H.; Luo, S.-W.; Tang, Z.; Cun, L.-F.; Mi, A.-Q.; Jiang, Y.-Z.; Gong, L.-Z. Organocatalyzed Highly Enantioselective Direct Aldol Reactions of Aldehydes with Hydroxyacetone and Fluoroacetone in Aqueous Media: The Use of Water To Control Regioselectivity. *Chem. - Eur. J.* **2007**, *13*, 689−701.
(17) Pihko, P. M.; Laurikainen, K. M.; Usano, A.; Nyberg, A. I.; Kaavi, J. A. Effect of additives on the proline-catalyzed ketone−aldehyde aldol reactions. *Tetrahedron* **2006**, *62*, 317−328.
(18) Seebach, D.; Beck, A. K.; Badine, D. M.; Limbach, M.; Eschenmoser, A.; Treasurywala, A. M.; Hobi, R.; Prikoszovich, W.; Linder, B. Are Oxazolidinones Really Unproductive, Parasitic Species in Proline Catalysis? − Thoughts and Experiments Pointing to an Alternative View. *Helv. Chim. Acta* **2007**, *90*, 425−471.
(19) Zotova, N.; Franzke, A.; Armstrong, A.; Blackmond, D. G. Clarification of the Role of Water in Proline-Mediated Aldol Reactions. *J. Am. Chem. Soc.* **2007**, *129*, 15100−15101.
(20) Ashley, M. A.; Hirschi, J. S.; Izzo, J. A.; Vetticatt, M. J. Isotope Effects Reveal the Mechanism of Enamine Formation in L-Proline-Catalyzed α-Amination of Aldehydes. *J. Am. Chem. Soc.* **2016**, *138*, 1756−1759.
(21) Evans, G.; Gibbs, T. J. K.; Jenkins, R. L.; Coles, S. J.; Hursthouse, M. B.; Platts, J. A.; Tomkinson, N. C. O. Kinetics of Iminium Ion Catalysis. *Angew. Chem., Int. Ed.* **2008**, *47*, 2820−2823.
(22) Nielsen, M.; Worgull, D.; Zweifel, T.; Gschwend, B.; Bertelsen, S.; Jørgensen, K. A. Mechanisms in aminocatalysis. *Chem. Commun.* **2011**, *47*, 632−649.
(23) Cheong, P. H.-Y.; Legault, C. Y.; Um, J. M.; Çelebi-Ölçüm, N.; Houk, K. N. Quantum Mechanical Investigations of Organocatalysis: Mechanisms, Reactivities, and Selectivities. *Chem. Rev.* **2011**, *111*, 5042−5137.
(24) Halskov, K. S.; Donslund, B. S.; Paz, B. M.; Jørgensen, K. A. Computational Approach to Diarylprolinol-Silyl Ethers in Aminocatalysis. *Acc. Chem. Res.* **2016**, *49*, 974−986.
(25) Walden, D. M.; Ogba, O. M.; Johnston, R. C.; Cheong, P. H. Computational Insights into the Central Role of Nonbonding Interactions in Modern Covalent Organocatalysis. *Acc. Chem. Res.* **2016**, *49*, 1279−1291.
(26) Ribas-Arino, J.; Carvajal, M. A.; Chaumont, A.; Masia, M. Unraveling the Role of Water in the Stereoselective Step of Aqueous Proline-Catalyzed Aldol Reactions. *Chem. - Eur. J.* **2012**, *18*, 15868−15874.

DOI: 10.1021/acs.jpca.7b11803
J. Phys. Chem. A 2018, 122, 451−459

(27) Hooper, J. F.; James, N. C.; Bozkurt, E.; Aviyente, V.; White, J. M.; Holland, M. C.; Gilmour, R.; Holmes, A. B.; Houk, K. N. Medium-Ring Effects on the Endo/Exo Selectivity of the Organocatalytic Intramolecular Diels−Alder Reaction. *J. Org. Chem.* **2015**, *80*, 12058−12075.
(28) Krenske, E. H.; Houk, K. N.; Harmata, M. Computational Analysis of the Stereochemical Outcome in the Imidazolidinone-Catalyzed Enantioselective (4 + 3)-Cycloaddition Reaction. *J. Org. Chem.* **2015**, *80*, 744−750.
(29) *Privileged Chiral Ligands and Catalysts*; Zhou, Q.-L., Ed.; Wiley-VCH Verlag GmbH & Co. KGaA: Weinheim, Germany, 2011.
(30) Holland, M. C.; Paul, S.; Schweizer, W. B.; Bergander, K.; Muck-Lichtenfeld, C.; Lakhdar, S.; Mayr, H.; Gilmour, R. Noncovalent interactions in organocatalysis: modulating conformational diversity and reactivity in the MacMillan catalyst. *Angew. Chem., Int. Ed.* **2013**, *52*, 7967−7971.
(31) Holland, M. C.; Gilmour, R. Deconstructing covalent organocatalysis. *Angew. Chem., Int. Ed.* **2015**, *54*, 3862−3871.
(32) Holland, M. C.; Metternich, J. B.; Daniliuc, C.; Schweizer, W. B.; Gilmour, R. Aromatic Interactions in Organocatalyst Design: Augmenting Selectivity Reversal in Iminium Ion Activation. *Chem. - Eur. J.* **2015**, *21*, 10031−10038.
(33) Donslund, B. S.; Johansen, T. K.; Poulsen, P. H.; Halskov, K. S.; Jørgensen, K. A. The Diarylprolinol Silyl Ethers: Ten Years After. *Angew. Chem., Int. Ed.* **2015**, *54*, 13860−13874.
(34) Erkkila, A.; Majander, I.; Pihko, P. M. Iminium catalysis. *Chem. Rev.* **2007**, *107*, 5416−5470.
(35) Mukherjee, S.; Yang, J. W.; Hoffmann, S.; List, B. Asymmetric enamine catalysis. *Chem. Rev.* **2007**, *107*, 5471−5569.
(36) Zhao, Y.; Truhlar, D. G. The M06 suite of density functionals for main group thermochemistry, thermochemical kinetics, noncovalent interactions, excited states, and transition elements: two new functionals and systematic testing of four M06-class functionals and 12 other functionals. *Theor. Chem. Acc.* **2008**, *120*, 215−241.
(37) Zhao, Y.; Truhlar, D. G. Density functionals with broad applicability in chemistry. *Acc. Chem. Res.* **2008**, *41*, 157−167.
(38) Lynch, B. J.; Zhao, Y.; Truhlar, D. G. Effectiveness of Diffuse Basis Functions for Calculating Relative Energies by Density Functional Theory. *J. Phys. Chem. A* **2003**, *107*, 1384−1388.
(39) Świderek, K.; Tuñón, I.; Marti, S.; Moliner, V.; Bertran, J. Role of solvent on nonenzymatic peptide bond formation mechanisms and kinetic isotope effects. *J. Am. Chem. Soc.* **2013**, *135*, 8708−8719.
(40) Świderek, K.; Martí, S.; Moliner, V. Theoretical Study of Primary Reaction of Pseudozyma antarctica Lipase B as the Starting Point To Understand Its Promiscuity. *ACS Catal.* **2014**, *4*, 426−434.
(41) Świderek, K.; Tuñón, I.; Marti, S.; Moliner, V. Protein Conformational Landscapes and Catalysis. Influence of Active Site Conformations in the Reaction Catalyzed by L-Lactate Dehydrogenase. *ACS Catal.* **2015**, *5*, 1172−1185.
(42) Krzeminska, A.; Moliner, V.; Świderek, K. Dynamic and Electrostatic Effects on the Reaction Catalyzed by HIV-1 Protease. *J. Am. Chem. Soc.* **2016**, *138*, 16283−16298.
(43) Świderek, K.; Pabis, A.; Moliner, V. A theoretical study of carbon-carbon bond formation by a Michael-type addition. *Org. Biomol. Chem.* **2012**, *10*, 5598−5605.
(44) Marenich, A. V.; Cramer, C. J.; Truhlar, D. G. Universal Solvation Model Based on Solute Electron Density and on a Continuum Model of the Solvent Defined by the Bulk Dielectric Constant and Atomic Surface Tensions. *J. Phys. Chem. B* **2009**, *113*, 6378−6396.
(45) McQuarrie, D. A. *Statistical Mechanics*; Harper & Row: New York, 1976.
(46) Reed, A. E.; Curtiss, L. A.; Weinhold, F. Intermolecular interactions from a natural bond orbital, donor-acceptor viewpoint. *Chem. Rev.* **1988**, *88*, 899−926.
(47) Frisch, M. J.; Trucks, G. W.; Schlegel, H. B.; Scuseria, G. E.; Robb, M. A.; Cheeseman, J. R.; Scalmani, G.; Barone, V.; Mennucci, B.; Petersson, G. A.; et al. *Gaussian09*; Gaussian. Inc.: Wallingford, CT, 2009.
(48) Evans, G. J. S.; White, K.; Platts, J. A.; Tomkinson, N. C. O. Computational study of iminium ion formation: effects of amine structure. *Org. Biomol. Chem.* **2006**, *4*, 2616−2627.
(49) Brazier, J. B.; Hopkins, G. P.; Jirari, M.; Mutter, S.; Pommereuil, R.; Samulis, L.; Platts, J. A.; Tomkinson, N. C. O. Iminium ion catalysis: direct comparison of imidazolidinone and diarylprolinol ether reactivity. *Tetrahedron Lett.* **2011**, *52*, 2783−2785.
(50) Brazier, J. B.; Jones, K. M.; Platts, J. A.; Tomkinson, N. C. On the roles of protic solvents in imidazolidinone-catalyzed transformations. *Angew. Chem., Int. Ed.* **2011**, *50*, 1613−1616.
(51) Bruvoll, M.; Hansen, T.; Uggerud, E. Organocatalysis: quantum chemical modeling of nucleophilic addition to α,β-unsaturated carbonyl compounds. *J. Phys. Org. Chem.* **2007**, *20*, 206−213.

DOI: 10.1021/acs.jpca.7b11803
J. Phys. Chem. A 2018, 122, 451−459